

RESEARCH

Open Access



Overexpression of *MtIPT* gene enhanced drought tolerance and delayed leaf senescence of creeping bentgrass (*Agrostis stolonifera* L.)

Ye Ai^{1,2,3}, Yinglong Chen³, Ning Wang⁴, Jiaying Li^{1,2}, Jinnan Liu^{1,2}, Liangying Shen^{1,2}, Xinbo Sun⁵, Liebao Han^{1,2*} and Yuehui Chao^{1,2*}

Abstract

Background Isopentenyltransferases (IPT) serve as crucial rate-limiting enzyme in cytokinin synthesis, playing a vital role in plant growth, development, and resistance to abiotic stress.

Results Compared to the wild type, transgenic creeping bentgrass exhibited a slower growth rate, heightened drought tolerance, and improved shade tolerance attributed to delayed leaf senescence. Additionally, transgenic plants showed significant increases in antioxidant enzyme levels, chlorophyll content, and soluble sugars. Importantly, this study uncovered that overexpression of the *MtIPT* gene not only significantly enhanced cytokinin and auxin content but also influenced brassinosteroid level. RNA-seq analysis revealed that differentially expressed genes (DEGs) between transgenic and wild type plants were closely associated with plant hormone signal transduction, steroid biosynthesis, photosynthesis, flavonoid biosynthesis, carotenoid biosynthesis, anthocyanin biosynthesis, oxidation-reduction process, cytokinin metabolism, and wax biosynthesis. And numerous DEGs related to growth, development, and stress tolerance were identified, including cytokinin signal transduction genes (*CRE1*, *B-ARR*), antioxidantase-related genes (*APX2*, *PEX11*, *PER1*), Photosynthesis-related genes (*ATPF1A*, *PSBQ*, *PETF*), flavonoid synthesis genes (*F3H*, *C12RT1*, *DFR*), wax synthesis gene (*MAH1*), senescence-associated gene (*SAG20*), among others.

Conclusion These findings suggest that the *MtIPT* gene acts as a negative regulator of plant growth and development, while also playing a crucial role in the plant's response to abiotic stress.

Keywords *MtIPT* gene, Creeping bentgrass, Drought tolerance, Plant hormones, Leaf senescence

*Correspondence:

Liebao Han

hanliebao@163.com

Yuehui Chao

chaoyuehui@bjfu.edu.cn

¹School of Grassland Science of Beijing Forestry University, Beijing, China

²Engineering and Technology Research Center for Sports Field and Slope Protection Turf, National Forestry and Grassland Administration, Beijing, China

³UWA School of Agriculture and Environment, The UWA Institute of Agriculture, The University of Western Australia, Perth, WA, Australia

⁴Shenzhen Tidyfield System Biotechnology Co., Ltd, Shenzhen, China

⁵College of Agronomy, State Key Laboratory of North China Crop Improvement and Regulation/Key Laboratory of Crop Growth Regulation of Hebei Province, Hebei Agricultural University, Baoding, China



© The Author(s) 2024. **Open Access** This article is licensed under a Creative Commons Attribution-NonCommercial-NoDerivatives 4.0 International License, which permits any non-commercial use, sharing, distribution and reproduction in any medium or format, as long as you give appropriate credit to the original author(s) and the source, provide a link to the Creative Commons licence, and indicate if you modified the licensed material. You do not have permission under this licence to share adapted material derived from this article or parts of it. The images or other third party material in this article are included in the article's Creative Commons licence, unless indicated otherwise in a credit line to the material. If material is not included in the article's Creative Commons licence and your intended use is not permitted by statutory regulation or exceeds the permitted use, you will need to obtain permission directly from the copyright holder. To view a copy of this licence, visit <http://creativecommons.org/licenses/by-nc-nd/4.0/>.

Background

Cytokinin (CK) is a small molecule plant hormone composed of N⁶-adenine derivatives, playing a crucial role in plant growth, development, and stress response [1, 2]. CKs commonly found in higher plants include N⁶- Δ^2 -isopentenyladenine (iP), trans-zeatin (tZ), cis-zeatin (cZ), and dihydro-zeatin (DHZ). In plants, CKs primarily exist in the forms of iP, tZ, and their nucleosides, nucleotides and glycosides [3]. The predominant forms of CKs vary significantly among different plants, tissues within the same plant, and various developmental stages [4].

Numerous studies have indicated a correlation between plant leaf senescence and CK content [4, 5]. Research by Zhang, et al. [6] elucidated the molecular mechanism of CK decline during leaf senescence, demonstrating that plants can regulate leaf senescence by modulating endogenous CK levels.

Isopentenyltransferase (IPT) is a crucial rate-limiting enzyme in CK synthesis, with the *IPT* gene first identified in *Agrobacterium tumefaciens* [7]. It can be classified into two classes based on substrate specificity: adenine phosphate-IPT (ATP/ADP-IPT) and transfer RNA-IPT (tRNA-IPT) [8, 9]. Overexpression of the *IPT* gene results in increased CK content [10]. Transgenic plants overexpressing *IPT* display varying degrees of CK syndrome, including reduced root growth, altered apical dominance, and changes in stem and leaf growth [11]. This gene not only affects plant growth and development but also responds to abiotic stress. For example, the COR15a promoter-*IPT* gene enhanced low temperature tolerance in sugarcane (*Saccharum officinarum*) [12], and regulated expression of the *IPT* gene in peanut (*Arachis hypogaea*) improved peanut's drought tolerance [13]. Overexpression of the *Agrobacterium tumefaciens IPT* gene in cotton (*Gossypium hirsutum*) improved salt tolerance and

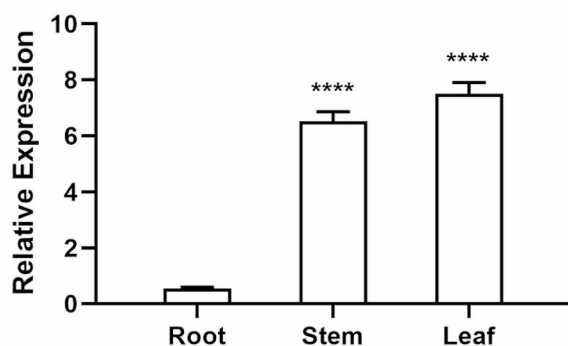


Fig. 1 QRT-PCR analysis of the relative expression of the *MtIPT* in different tissues of transgenic plant. Data represent the average from four biological replicates. Data are shown as means and the error bars indicate the standard deviation (\pm SD). Compared with root, significant difference was indicated with asterisks (ns, *, **, *** or ****) at ns, $P < 0.05$, 0.01, 0.001 or 0.0001 by Student's t-test

delayed senescence of cotton leaves [14]. Although *IPT* genes in *Agrobacterium tumefaciens* and plants have been widely studied, comprehensive research on the regulation mechanism of the *IPT* gene is still lacking.

Our laboratory, *Medicago truncatula* was treated with 6-benzylaminopurine (6-BA) and lovastatin, and several key regulatory genes potentially involved in CK response were screened using high-throughput sequencing, including the CK synthesis regulatory gene *MtIPT*. The *IPT* gene of *M. truncatula* was cloned using PCR, and the *MtIPT* gene was found to respond to drought stress.

Creeping bentgrass (*Agrostis stolonifera*) is a cold-season turf grass known for its ability to grow new roots and stems via stolons. Despite its soft grass color, rapid growth, salt tolerance, cold resistance, and resilience to low mowing and foot traffic, creeping bentgrass exhibits relatively weak drought tolerance [15]. Genetic transformation technology has been well developed for creeping bentgrass with high conversion efficiency. Compared with the wild type (WT), phenotypic changes in transgenic (OE) creeping bentgrass are easily observable, which facilitates the study of gene function. Due to difficulties in seed production and its genetic characteristics of self-incompatibility, traditional breeding methods struggle to genetically improve creeping bentgrass [16]. Therefore, genetic engineering has become a focal point for enhancing creeping bentgrass. It is hoped that superior germplasm resources of creeping bentgrass can be obtained through the introduction and screening of exogenous genes.

The purpose of this study is to explore the regulatory mechanism of the *MtIPT* gene on the growth and abiotic stress response of creeping bentgrass through gene transformation and overexpression. Building upon previous studies [17, 18], this research investigates various aspects of the *MtIPT* gene's regulatory mechanism, such as cell structure and hormone interactions. This study offers a new perspective for comprehensively understanding *IPT* gene function and CK regulation, laying a foundation for developing new varieties of creeping bentgrass.

Results

The acquisition of transgenic plants

The *MtIPT* gene (XM_003590629.4), 903 bp, was cloned via PCR (Fig. S1). Subsequently, the *MtIPT* gene was integrated into the genome of creeping bentgrass through agrobacterium-mediated transformation, resulting in 32 OE plants. The transcription of *MtIPT* in OE plants was confirmed by qRT-PCR. As depicted in Figure S2, *MtIPT* was effectively transcribed in creeping bentgrass. Moreover, the expression of the *MtIPT* gene was significantly higher in the leaf (13.5-fold) and stem (12.3-fold) tissues compared with the root section of transgenic creeping bentgrass (Fig. 1). Therefore, the above-ground portion

of transgenic creeping bentgrass was selected as the primary material for subsequent study.

Subcellular localization

The *MtIPT* gene was ligated into the 3302Y vector containing yellow fluorescent protein gene (*YFP*) and introduced into tobacco leaves via agrobacterium-mediated transformation. Using confocal laser microscopy, the isopentenyltransferase encoded by *MtIPT* was observed to localize in the cell membrane and nucleus (Fig. 2).

Phenotype and internal structure characteristics of wild-type and transgenic creeping bentgrass

WT and OE plants matured after 12 weeks of cultivation in soil (Fig. 3A). Compared with WT, OE plants exhibited significantly reduced stem length (26%) (Fig. 3B), shorter roots (40%) (Fig. 3C), and thinner leaves (47%) (Fig. 3D), while displaying a notably higher chlorophyll content (33%) (Fig. 3E). Interestingly, the tips of some leaves appeared red (Fig. 3A). Staining results from cross-sections indicated no discernible difference in leaf cell structure between WT and OE plants (Fig. 3F). However, scanning electron microscopy (SEM) results revealed that the content of wax crystals on the surface of stomata (Fig. 3G) was significantly higher in OE plants compared with WT. This enhancement may assist OE plants in reducing transpiration and retaining more water during periods of drought.

Response of *MtIPT* gene to drought stress

Four *M. truncatula* plants were treated with drought using 20% (w/v) Polyethylene glycol (PEG-6000). The results indicated that the expression of the *MtIPT* gene

initially increased, peaked at 8 h, and then decreased within 24 h. However, compared with the baseline (0 h), the expression of the *MtIPT* gene showed significant increases at 0.5 h (1.9-fold), 1 h (7.1-fold), 2 h (6.8-fold), 4 h (8.5-fold), 6 h (12.0-fold), 8 h (13.1-fold), 12 h (7.4-fold), and 24 h (4.6-fold) (Fig. 4). This indicates that the *MtIPT* gene responds to drought stress.

MtIPT gene enhances drought resistance of creeping bentgrass by increasing antioxidant enzymes

WT and OE plants were cultured under identical conditions, and plants in similar physiological states were selected for drought treatment (Fig. 5A). By the 14th day of drought treatment, the leaves of WT plants had significantly yellowed and some had withered, whereas the OE plants remained green (Fig. 5B). By the 22nd day, WT plants had experienced extensive leaf death, whereas the transgenic plants only showed partial wilting, with most leaves remaining green (Fig. 5C).

The contents of chlorophyll, antioxidant enzymes, and soluble sugars in the leaves of WT and OE plants were measured after 0 and 14 days of natural drought treatment. Following drought treatment, compared with WT plants, the peroxidase (POD) (77%), superoxide dismutase (SOD) (16%), and ascorbate peroxidase (APX) (28%) contents of OE plants significantly increased (Fig. 5D-F), while the malondialdehyde (MDA) content noticeably decreased (8%) (Fig. 5G). Additionally, the soluble sugar content increased significantly (17%) (Fig. 5H). Furthermore, the chlorophyll content in the leaves of OE plants was significantly higher (47%) than that in WT plants after drought treatment (Fig. 5I). These results indicate that overexpression of the *MtIPT* gene enhances

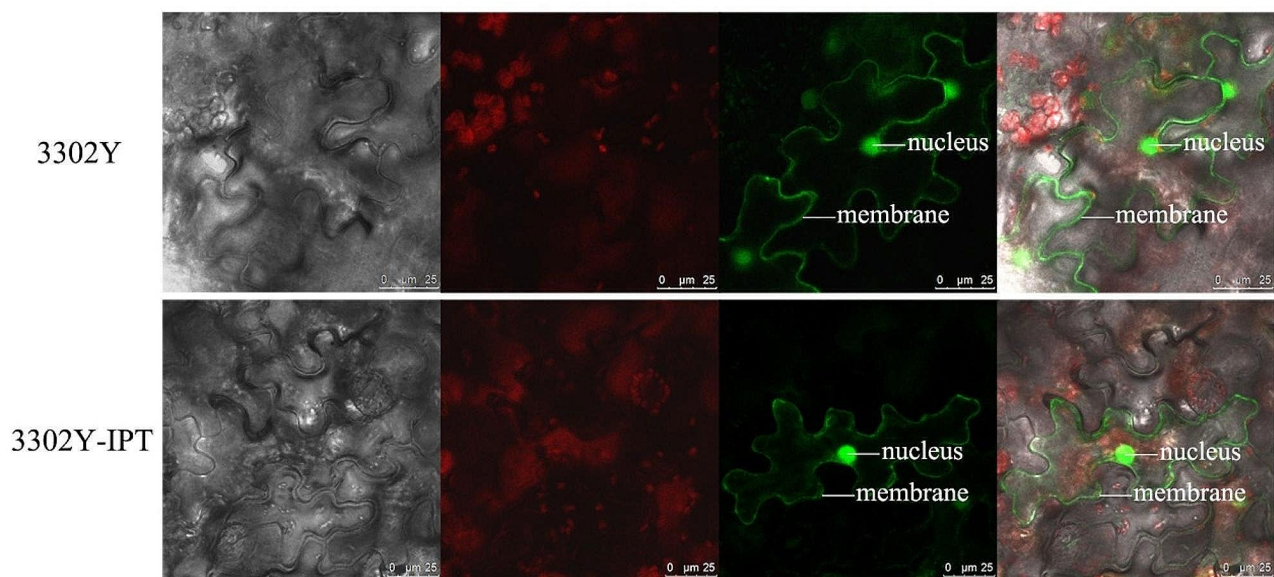


Fig. 2 Subcellular localization of *MtIPT* protein. 3302Y, control with empty vector. 3302Y-IPT, *MtIPT*-GFP fusion. Bars = 25 μ m

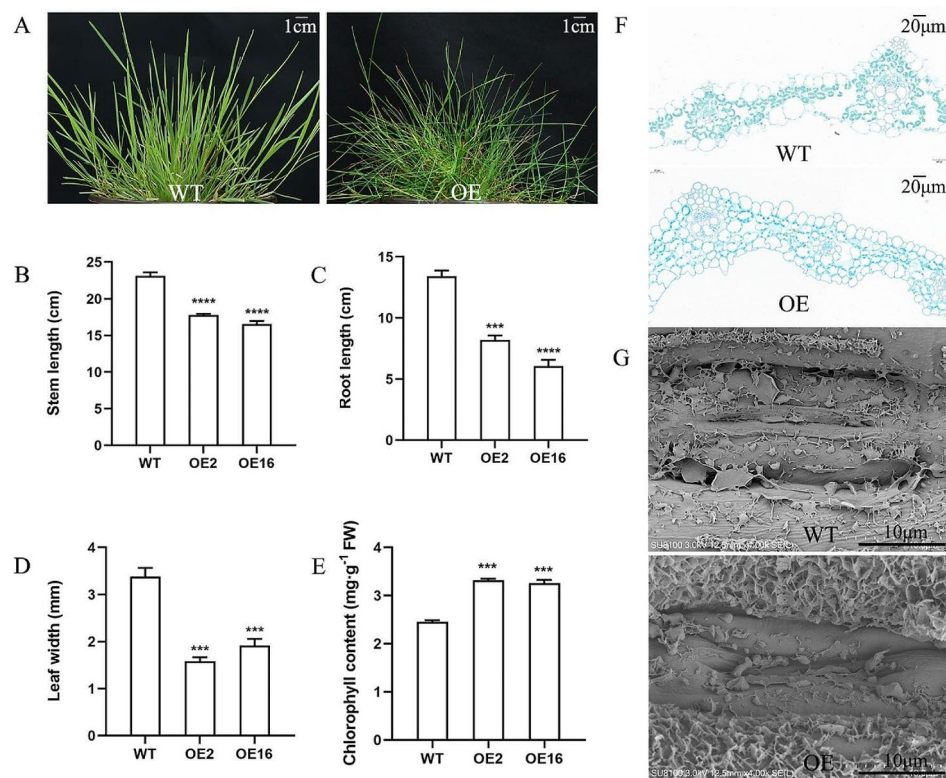


Fig. 3 Phenotypic characteristics, microstructure and chlorophyll content of plants. **(A)** Wild-type (WT) plants and transgenic (OE) plants were grown in soil (Nutrient soil: vermiculite: perlite=1:1:1) separately and photographed after maturity. **(B)** Statistical analysis of the differences in stem length, **(C)** root length, **(D)** leaf width and chlorophyll content **(E)** between representative WT and OE plants. Data represent the average from three biological replicates. Data are means of three biological replicates \pm standard deviation (SD). OE lines compared with WT, significant difference was indicated with asterisks (ns, *, **, *** or ****) at ns, $P < 0.05$, 0.01, 0.001 or 0.0001 by Student's t-test. **(F)** Cross sections of leaves of WT and OE plants. **(G)** Scanning electron microscope images of stomata of WT and OE leaves

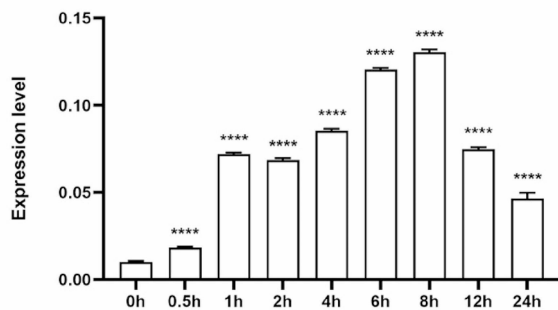


Fig. 4 The expression levels of *MtIPT* gene were analyzed at 0 h, 0.5 h, 1 h, 2 h, 4 h, 6 h, 8 h, 12 h, 24 h through drought treatment on healthy *Medicago truncatula*. Data represent the average from four biological replicates. Data are shown as means and the error bars indicate the standard deviation (\pm SD). Compared with 0 h, significant difference was indicated with asterisks (ns, *, **, *** or ****) at ns, $P < 0.05$, 0.01, 0.001 or 0.0001 by Student's t-test

the drought tolerance of creeping bentgrass by influencing its antioxidant capacity, photosynthetic performance, and osmotic regulation.

Transgenic plants improve shading by reducing the degradation of chlorophyll in leaves

The leaves of WT and OE plants were placed in 3 mM 2-Morpholinoethanesulphonic acid (MES) solution for dark culture (Fig. 6A). After 5 days, the leaves of WT plants showed slight yellowing, while those of OE plants exhibited minimal change (Fig. 6B). By day 8, the leaves of WT plants had almost completely yellowed, whereas those of OE plants only showed partial yellowing (Fig. 6C). Chlorophyll determination results indicated that the chlorophyll content in OE plants was significantly higher (83% and 63%) than in WT plants on days 5 and 8 (Fig. 6D). This demonstrates that the *MtIPT* gene can enhance plant shade tolerance by reducing chlorophyll degradation and delaying leaf senescence.

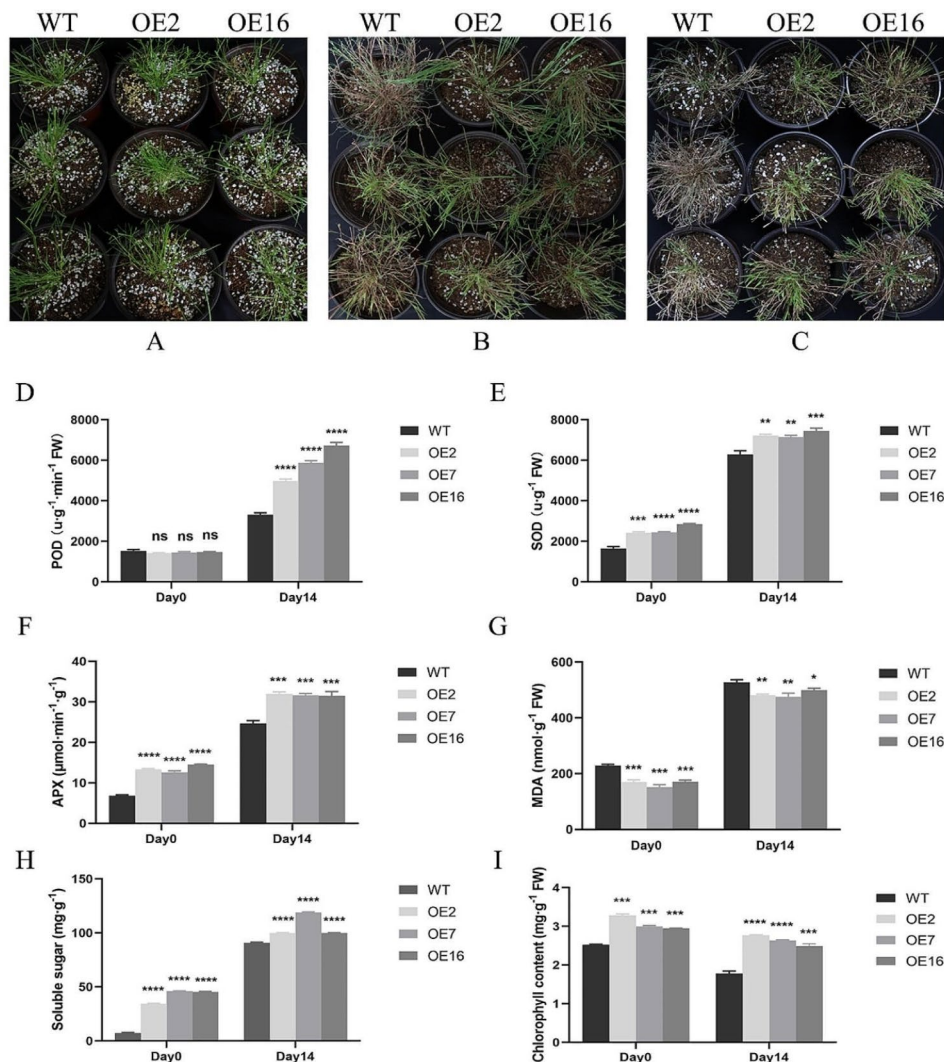


Fig. 5 Drought treatment of wild type (WT) and transgenic (OE) plants. Comparison of morphology of WT and OE plants under drought treatment at day 0 (A), day14 (B), day 22 (C). Physiological indexes of WT and OE plants were measured before (day 0) and after (day 14) drought treatment, including peroxidase (POD) (D), super oxide dimutase (SOD) (E), ascorbate peroxidase (APX) (F), malondialdehyde (MDA) (G), soluble sugar (H) and chlorophyll content (I). Data represent the average from three biological replicates. Data are shown as means and the error bars indicate the standard deviation (\pm SD). OE lines compared with WT, significant difference was indicated with asterisks (ns, *, **, *** or ****) at ns, $P < 0.05$, 0.01, 0.001 or 0.0001 by Student's t-test

Hormonal changes of transgenic creeping bentgrass

The hormone determination results revealed that overexpression of the *MtIPT* gene in creeping bentgrass led to an increase in CK trans-zeatin-riboside (88%) (Fig. 7D) and isopentenyl adenosine (35%) (Fig. 7F) content. Conversely, the CK DL-dihydrozeatin riboside content decreased (13%) (Fig. 7E), indicating that the *MtIPT* gene primarily catalyzed the synthesis of isopentenyl adenosine and trans-zeatin-riboside. Additionally, besides the significant changes in CK content, overexpression of *MtIPT* notably increased the levels of auxin (26%) (Fig. 7A), brassinosteroid (59%) (Fig. 7G), and abscisic acid (8%) (Fig. 7B) in OE plants. It also reduced the content of the hormone methyl jasmonate (34%) (Fig. 7H). These results suggest that various hormones co-regulate

the changes in growth, development, and abiotic stress response in OE plants. Compared with WT plants, the GA3 content in OE plants remained almost unchanged (Fig. 7C).

Epibrassinolide promotes the expression of *MtIPT* gene

According to the results of hormone determination, we found that overexpression of the *MtIPT* gene resulted in a significant increase in brassinosteroid content (Fig. 7G). It is intriguing to explore whether this increase in brassinosteroid content could also enhance the expression of *MtIPT*. Therefore, 24-epibrassinolide (EBR) was used for exogenous spraying. After EBR treatment, *MtIPT* gene expression was measured at different time points. As depicted in Fig. 8, compared with 0 h, *MtIPT* gene

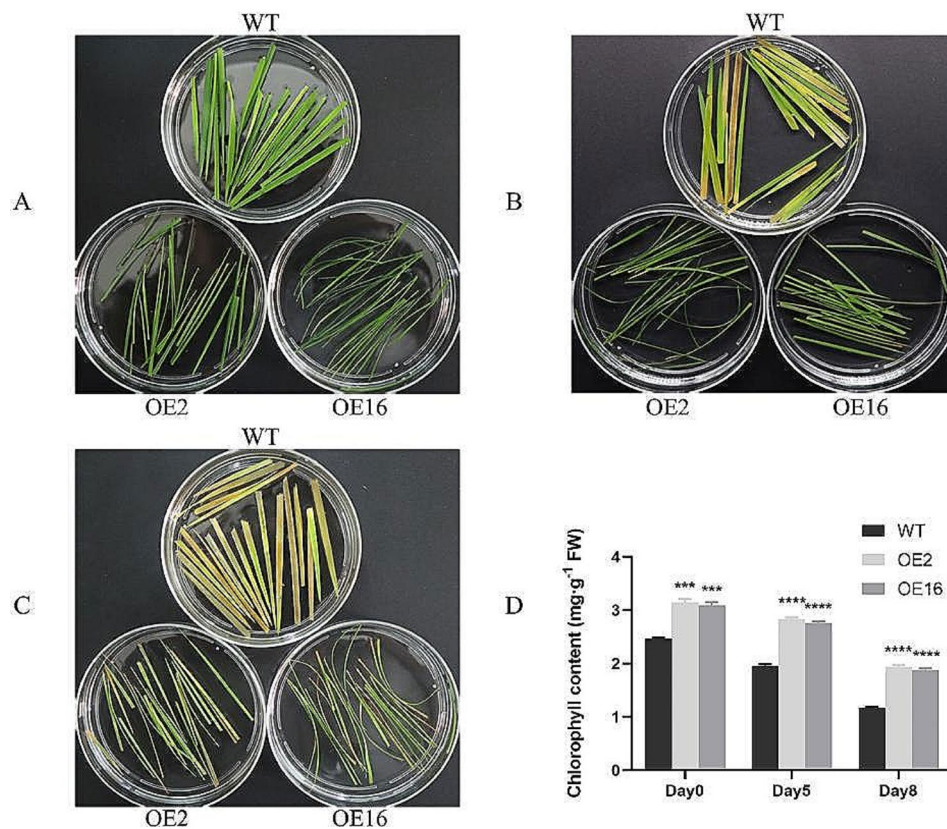


Fig. 6 Shade treatment of wild type (WT) and transgenic (OE) plants. WT, OE2 and OE16 leaves with the same growth state were selected from three plants respectively as three biological repeat samples. The leaves of WT and OE plants were darkened in 3 mM 2-Morpholinoethanesulphonic acid (MES) solution, and the state of the leaves was recorded by photos on day 0 (**A**), day 5 (**B**) and day 8 (**C**). **D** Chlorophyll content of WT and OE plants before and after shading treatment. Data represent the average from three biological replicates. Data are shown as means and the error bars indicate the standard deviation (\pm SD). OE lines compared with WT, significant difference was indicated with asterisks (ns, *, **, *** or ****) at ns, $P < 0.05$, 0.01, 0.001 or 0.0001 by Student's t-test

expression was up-regulated at 0.5 h (1.1-fold), 1 h (1.7-fold), 6 h (1.4-fold), 9 h (1.1-fold), 12 h (1.5-fold), and 24 h (2.7-fold), illustrating that the elevated concentration of exogenous EBR also contributed to improving the expression level of the *MiIPT* gene. Consequently, it is suggested that there is a certain synergistic effect between cytokinin and brassinosteroid, and they participate in regulating plant life processes through interaction.

Results of transcriptome sequencing

High-throughput sequencing was conducted to investigate changes in growth, development, and abiotic stress response in OE plants. A total of 39.33 Gb of clean data were obtained, with all samples yielding 6.37Gb of clean data and a Q30 base percentage of 93.57% or higher (Table 1). A total of 72,209 unigenes were assembled, with an N50 of 1,697. Additionally, 36,452 unigenes were annotated following comparison with multiple databases. Differentially expressed genes (DEGs) were identified based on their expression levels across different samples. In transgenic creeping bentgrass compared with WT,

8,700 DEGs were identified, with 4,122 up-regulated and 4,578 down-regulated genes.

Based on GO analysis, the main enriched biological processes of up-regulated DEGs include triterpenoid biosynthetic process, glycogen biosynthetic process, brassinosteroid metabolic process, inositol biosynthetic process, neutral lipid biosynthetic process, inositol phosphate-mediated signaling, oxidation-reduction process, cytokinin metabolic process, brassinosteroid homeostasis, steroid biosynthetic process, among others. The main enriched biological processes of down-regulated DEGs include cell surface receptor signaling pathway, DNA integration, plant-type secondary cell wall biogenesis, mitochondrial calcium ion transmembrane transport, RNA-dependent DNA biosynthetic process, regulation of mitotic spindle organization, sterol metabolic process, de novo protein folding, regulation of intracellular signal transduction, simple leaf morphogenesis, among others (Fig. 9A) (Tables S1, S2, S3). These processes may be closely related to the slower growth observed in OE plants.

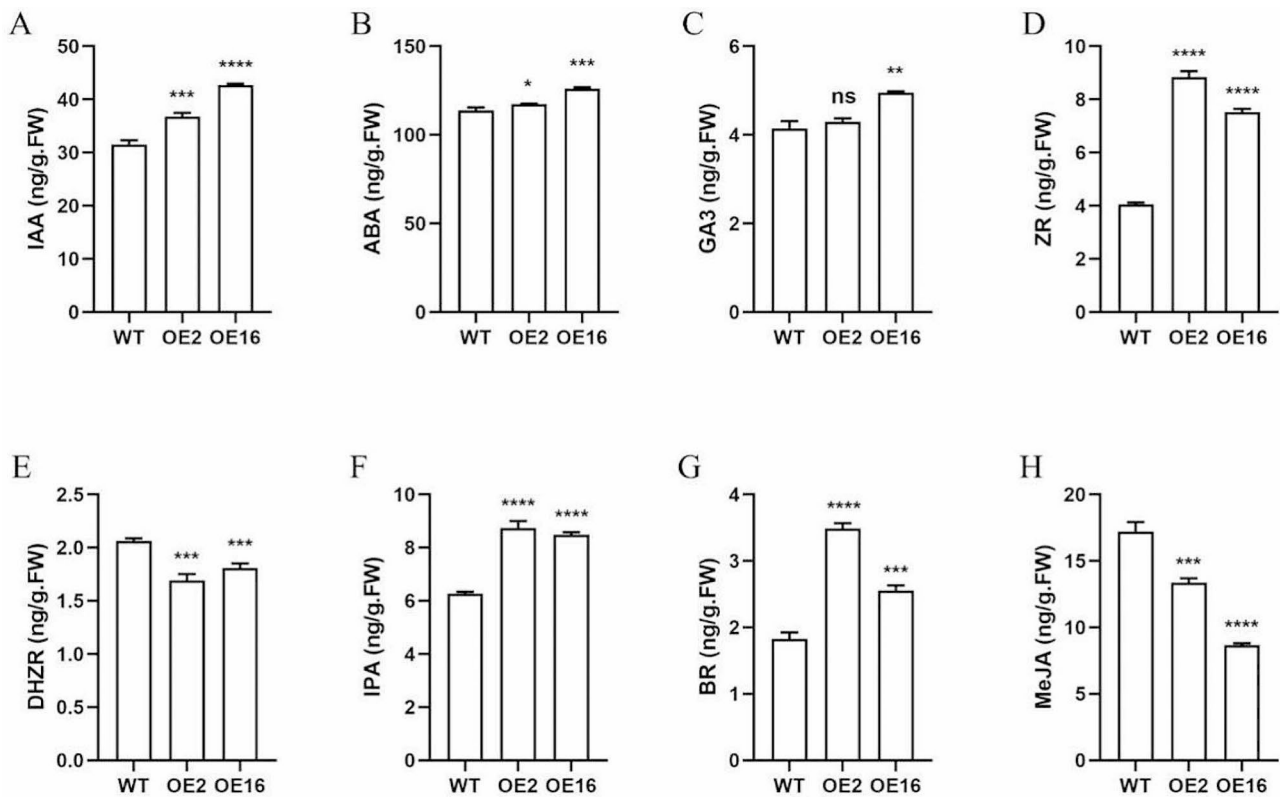


Fig. 7 Hormone content in the ground parts of wild type (WT) and transgenic (OE) plants. **A** Auxin (IAA) content. **B** Abscisic acid (ABA) content. **C** Gibberellin 3 (GA3) content. **D** Cytokinin trans-Zeatin-riboside (ZR) content. **E** Cytokinin DL-dihydrozeatin riboside (DHZR) content. **F** Cytokinin isopentenyl adenosine (IPA) content. **G** Brassinosteroid (BR) content. **H** methyl jasmonate (MeJA) content. The unit is ng/g. FW. Data represent the average from three biological replicates. Data are shown as means and the error bars indicate the standard deviation (\pm SD). OE lines compared with WT, significant difference was indicated with asterisks (ns, *, **, *** or ****) at ns, $P < 0.05$, 0.01, 0.001 or 0.0001 by Student's t-test

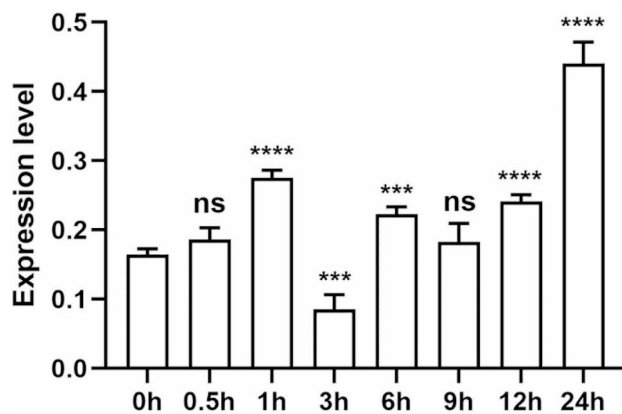


Fig. 8 The expression levels of *MtiPT* gene were analyzed at 0 h, 0.5 h, 1 h, 3 h, 6 h, 9 h, 12 h, 24 h after exogenous application of 0.1 μ mol 24-epibrassinolide (EBR) on healthy *Medicago truncatula*. Data represent the average from four biological replicates. Data are shown as means and the error bars indicate the standard deviation (\pm SD). Compared with 0 h, significant difference was indicated with asterisks (ns, *, **, *** or ****) at ns, $P < 0.05$, 0.01, 0.001 or 0.0001 by Student's t-test

Table 1 Data quality of RNA-Seq in wild-type and transgenic creeping bentgrass

BMK-ID	Read Number	Base Number	GC Content	% \geq Q30
WT1	22,102,451	6,616,446,434	54.30%	93.79%
WT2	22,134,526	6,626,966,790	54.79%	94.03%
WT3	22,389,789	6,702,563,848	54.16%	93.57%
OE1	21,271,848	6,370,559,282	53.50%	93.60%
OE2	21,731,416	6,504,895,292	53.57%	93.58%
OE3	21,750,388	6,513,295,706	53.68%	93.62%

Note WT: wild-type plant. OE: transgenic plant. Read Number: Total number of pair-end Reads in clean data. Base Number: The total number of bases in clean data. GC Content: GC content in clean data, that is, the percentage of G and C bases in the total base in clean data. % \geq Q30: The percentage of bases with a mass value greater than or equal to 30 in clean data

The main enriched cellular components of up-regulated DEGs include lipid droplet, obsolete axoneme part, integral component of chloroplast outer membrane, chloroplast stroma, extrinsic component of mitochondrial inner membrane, and peptidase complex, among others. Conversely, the main enriched cellular components of down-regulated DEGs include apoplast, extracellular region, spindle, cell wall, spindle microtubule, microtubule, and integral component of plasma membrane, among others (Fig. 9B) (Tables S4, S5, S6).

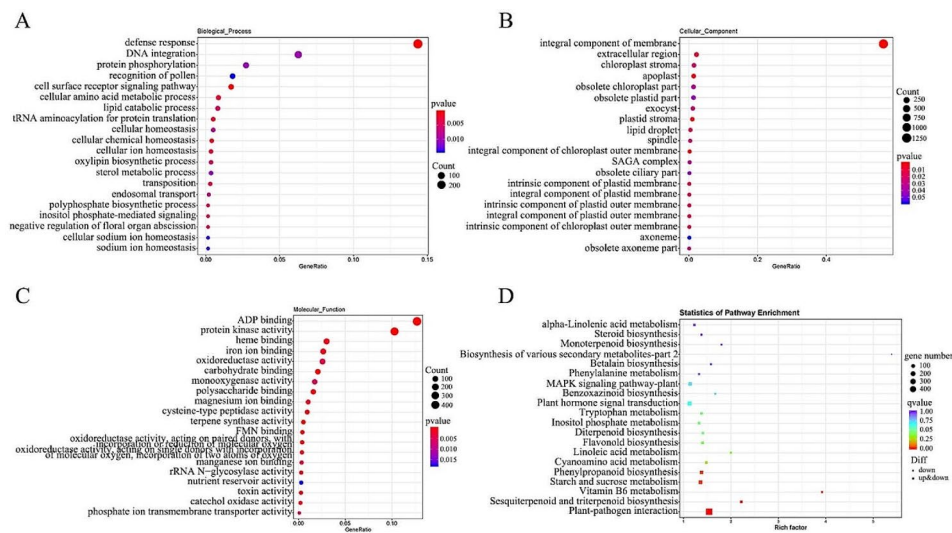


Fig. 9 Global analysis of gene expression between wild type (WT) and transgenic (OE) plants. **A** The biological process analysis of Gene Ontology (GO) enrichment of the all annotated differentially expressed genes (DEGs) in OE-vs-WT group. **B** The cellular component analysis of GO enrichment of the all annotated DEGs in OE-vs-WT group. **C** The molecular function analysis of GO enrichment of the all annotated DEGs in OE-vs-WT group. Note: OE-vs-WT: transgenic plants verse wild type plants. 20 most significant GO categories were selected according to the pvalue. **D** Kyoto Encyclopedia of Genes and Genomes (KEGG) analysis of the annotated DEGs in OE-vs-WT group. Note: OE-vs-WT: transgenic plants verse wild type plants. 20 most significant KEGG pathways were selected according to the qvalue. Note: GeneRatio: Ratio of the number of genes associated with the category/pathway among the genes used for enrichment analysis to the total number of genes used for enrichment analysis. A higher ratio indicates that more DEGs are enriched in this category/pathway. Enrichment factor: A parameter that reflects gene enrichment, indicating the ratio of the proportion of genes annotated to an category/pathway in DEGs to the proportion of genes annotated to that category/pathway in all genes. A larger enrichment factor indicates that the enrichment level of DEGs in this category/pathway is more significant. Pvalue: Statistically significant levels for enrichment analysis. qvalue is the pvalue after correction for multiple hypothesis testing. The smaller qvalue indicates that the enrichment significance of DEGs in this category/pathway is more reliable. The size of the circle indicates the number of genes enriched in the category/pathway

The main enriched molecular functions of up-regulated DEGs include oxidoreductase activity, lanosterol synthase activity, transaminase activity, 1,4-alpha-glucan branching enzyme activity, phosphoric diester hydrolase activity, and cytokinin dehydrogenase activity, among others. On the other hand, the main enriched molecular functions of down-regulated DEGs include ADP binding, protein kinase activity, polysaccharide binding, threonine synthase activity, monooxygenase activity, and DNA-binding transcription factor activity, among others (Fig. 9C) (Tables S7, S8, S9).

KEGG analysis revealed that DEGs were predominantly involved in pathways such as terpenoid biosynthesis, starch and sucrose metabolism, phenylpropanoid biosynthesis, linoleic acid metabolism, flavonoid biosynthesis, tryptophan metabolism, inositol phosphate metabolism, plant hormone signal transduction, MAPK signaling pathway-plant, steroid biosynthesis, betalain biosynthesis, photosynthesis, anthocyanin biosynthesis, brassinosteroid biosynthesis, cutin, suberine and wax biosynthesis, carotenoid biosynthesis, and zeatin biosynthesis, among others (Fig. 9D).

The phenotypes observed in OE plants prompted us to focus on DEGs associated with plant growth and stress response to elucidate the molecular mechanisms of *MtIPT*-mediated alterations in plant development

and stress resistance. Given the slow growth phenotype observed in aboveground parts and roots of OE plants, biological pathways related to auxin and roots were analyzed in OE plants, including microtubule-associated proteins (MAPs), auxin response factors (ARFs), indoleacetic acid-induced proteins (IAAs), SMALL AUXIN UP RNA (SAUR), auxin transporter-like proteins (AUX1), and IAA-amino acid hydrolase ILR1-like proteins (ILR1). These genes showed both up-regulation (10 unigenes) and down-regulation (14 unigenes) in OE plants. Simultaneously, a significant number of stress-related candidate genes were identified (Table 2). Additionally, 8 functional genes were selected for verification of their expression levels, which were consistent with the expression profiles observed in the RNA-seq data (Fig. 10A-H).

Discussion

IPT is a key rate-limiting enzyme in CK synthesis, and numerous studies have demonstrated its close association with plant growth and development. Sa, et al. [19] found that overexpression of the *IPT* gene altered endogenous CK levels, affecting plant morphology, floral organ systems, and reproductive processes. Similarly, transgenic *GmIPT* tobacco (*Nicotiana tabacum*) showed inhibited root and aboveground growth, shortened internodes, thicker phenotypes, and darker green leaves [20]. In this

Table 2 Annotation of selected genes associated with stress tolerance

Pathway or Category	Gene ID	Annotation	log ₂ FC
Wax biosynthesis	c82850.graph_c0	Midchain alkane hydroxylase	4.142
Carotenoid biosynthesis	c106813.graph_c0	15-cis-phytoene synthase	1.124
Carotenoid biosynthesis	c94504.graph_c2	15-cis-phytoene synthase	4.164
Carotenoid biosynthesis	c95444.graph_c0	β-carotene 3-hydroxylase	1.089
Steroid biosynthesis	c98984.graph_c0	Cycloartenol synthase	3.605
Steroid biosynthesis	c100386.graph_c0	Sterol 24-C-methyltransferase	1.012
Steroid biosynthesis	c92136.graph_c4	plant 3β-hydroxysteroid-4α-carboxylate 3-dehydrogenase	2.281
Brassinosteroid biosynthesis	c98550.graph_c0	Brassinosteroid C-23 hydroxylase	1.528
Flavonoid biosynthesis	c98017.graph_c0	Naringenin 3-dioxygenase	6.531
Flavonoid biosynthesis	c88881.graph_c3	Flavanone 7-O-glucoside 2"-O-beta-L-rhamnosyltransferase	4.028
Flavonoid biosynthesis	c107378.graph_c0	Bifunctional dihydroflavonol 4-reductase/flavanone 4-reductase	1.490
Flavonoid biosynthesis	c99560.graph_c0	Anthocyanidin synthase	2.594
Anthocyanidin biosynthesis	c66067.graph_c0	Anthocyanidin 3-O-glucosyltransferase-like	6.825
Anthocyanidin biosynthesis	c71336.graph_c0	Anthocyanidin 3-O-glucosyltransferase	4.325
Peroxisome	c101747.graph_c0	Peroxin-6	2.915
Peroxisome	c89281.graph_c0	Peroxin-11	1.024
Peroxisome	c87908.graph_c0	Peroxin-14	2.724
Peroxisome	c89896.graph_c0	L-ascorbate peroxidase 2	1.171
Peroxisome	c98145.graph_c0	Peroxidase 16	1.629
Peroxisome	c95178.graph_c2	Peroxidase 1	1.841
Oxidoreductase activity	c94252.graph_c1	Peroxisomal (S)-2-hydroxy-acid oxidase	1.523
Oxidoreductase activity	c105281.graph_c1	Peroxisomal (S)-2-hydroxy-acid oxidase	1.112
Oxidoreductase activity	c94252.graph_c0	Peroxisomal (S)-2-hydroxy-acid oxidase	1.319
Photosynthesis	c91998.graph_c0	F-type H ⁺ -transporting ATPase subunit alpha	2.661
Photosynthesis	c96696.graph_c0	F-type H ⁺ /Na ⁺ -transporting ATPase subunit alpha	1.324
Photosynthesis	c89036.graph_c0	Photosystem II oxygen-evolving enhancer protein 3	1.057
Photosynthesis	c94120.graph_c1	Photosystem II oxygen-evolving enhancer protein 3	1.061
Photosynthesis	c70027.graph_c1	Ferredoxin	4.729
Photosynthesis	c91338.graph_c0	Cytochrome c6	1.248
Cytokinin signal transduction	c107619.graph_c0	Arabidopsis histidine kinase 2/3/4 (cytokinin receptor)	-1.092
Cytokinin signal transduction	c108647.graph_c2	Arabidopsis histidine kinase 2/3/4 (cytokinin receptor)	-6.664
Cytokinin signal transduction	c89363.graph_c0	Arabidopsis histidine kinase 2/3/4 (cytokinin receptor)	-5.626
Cytokinin signal transduction	c102073.graph_c2	Two-component response regulator ARR-B family	-1.173
Cytokinin signal transduction	c107195.graph_c1	Two-component response regulator ARR-B family	-1.006
Cytokinin signal transduction	c93497.graph_c0	Two-component response regulator ARR-B family	-1.364
Cytokinin signal transduction	c95989.graph_c0	Two-component response regulator ARR-B family	-1.319
Cytokinin signal transduction	c102520.graph_c0	Two-component response regulator ARR-B family	1.614
Cytokinin signal transduction	c99367.graph_c1	Two-component response regulator ARR-A family	1.147
Plant organ senescence	c97285.graph_c1	Senescence associated gene 20	-1.108
Monooxygenase activity	c102404.graph_c0	Cytochrome P450 89A9	-4.509
Starch and sucrose metabolism	c99603.graph_c0	Hexokinase-9	1.402

Note Log₂FC: log₂ fold change (FC) value of DEGs

study, overexpression of *MtIPT* in creeping bentgrass led to slower growth in aboveground parts and roots, with darker leaf color, consistent with findings by Ye, et al. [20]. GO analysis from high-throughput sequencing revealed that down-regulated DEGs were enriched in biological processes such as DNA integration, plant-type secondary cell wall biogenesis, mitochondrial calcium ion transmembrane transport, RNA-dependent DNA biosynthesis, regulation of mitotic spindle organization, protein folding, and regulation of intracellular signal

transduction. These findings suggest that *MtIPT* may retard plant growth by influencing DNA replication and protein synthesis to some extent.

The *MtIPT* gene not only influences growth and development but also regulates plant response to abiotic stress. Various studies have shown that *IPT* genes in plants respond to stresses like high temperature [21], low temperature [12], drought [17], and salt [22]. Through high-throughput sequencing, Xu, et al. [23] found differential expression of receptor kinase, stress

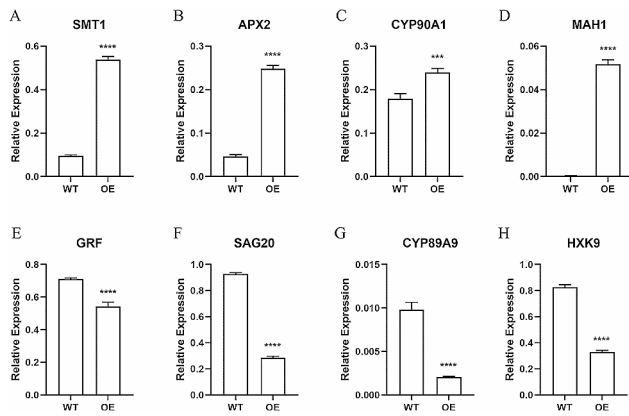


Fig. 10 Relative expression of the selected DEGs (A-H) determined by qRT-PCR. Data represent the average from four biological replicates. Data are shown as means and the error bars indicate the standard deviation (\pm SD). Significant differences between the two samples were indicated with asterisks (ns, *, **, *** or ****) at ns, $P < 0.05, 0.01, 0.001$ or 0.0001 by Student's t -test

defense, protein modularization, and protein degradation genes between transgenic *IPT* and wild-type plants under drought stress. In this study, overexpression of *MtIPT* enhanced drought tolerance and shade tolerance in creeping bentgrass by delaying leaf senescence. High-throughput sequencing also highlighted DEGs related to plant hormone signal transduction, steroid biosynthesis, photosynthesis, flavonoid biosynthesis, carotenoid biosynthesis, anthocyanin biosynthesis, oxidation-reduction process, cytokinin metabolism, and wax biosynthesis in OE plants compared with WT.

Drought can increase the levels of O^- and H_2O_2 levels in plant tissues, inducing rapid accumulation of reactive oxygen species (ROS) and oxidative damage to proteins and lipids [24, 25]. Plants have developed defense mechanisms to regulate ROS levels, including antioxidant enzymes like POD, SOD [26], and non-enzymatic antioxidants such as flavonoids [27, 28]. In this study, OE plants showed significantly up-regulated expression of antioxidant genes (*APX2*, *PEX11*, and *PER1*), higher levels of antioxidant enzymes (POD, SOD, APX), lower levels of malondialdehyde (MDA), and increased expression of flavonoid synthesis genes (*F3H*, *C12RT1*, *DFR*) compared with WT. These results indicate that the *MtIPT* gene enhances drought tolerance in OE plants by improving antioxidant capacity.

Anthocyanins are also a kind of flavonoids, which act as effective and broad-spectrum protective compounds and can accumulate in vacuoles, functioning as osmotic regulators to improve plant drought tolerance [29]. Nogues, et al. [30] found that UV-B-induced anthocyanins reduced pea (*Pisum sativum*) damage under drought stress, enhancing drought tolerance. The *BZ1* gene, encoding anthocyanidin 3-O-glucosyltransferase, is responsible for anthocyanin synthesis [31]. ANS is a key enzyme at the end of plant anthocyanin biosynthesis pathway [32]. In this study, *BZ1* and *ANS* genes were significantly up-regulated in OE plants. This suggests that overexpression of the *MtIPT* gene increases anthocyanin content by promoting the up-regulation of *BZ1* and *ANS*, thereby reducing drought-induced damage to OE plants.

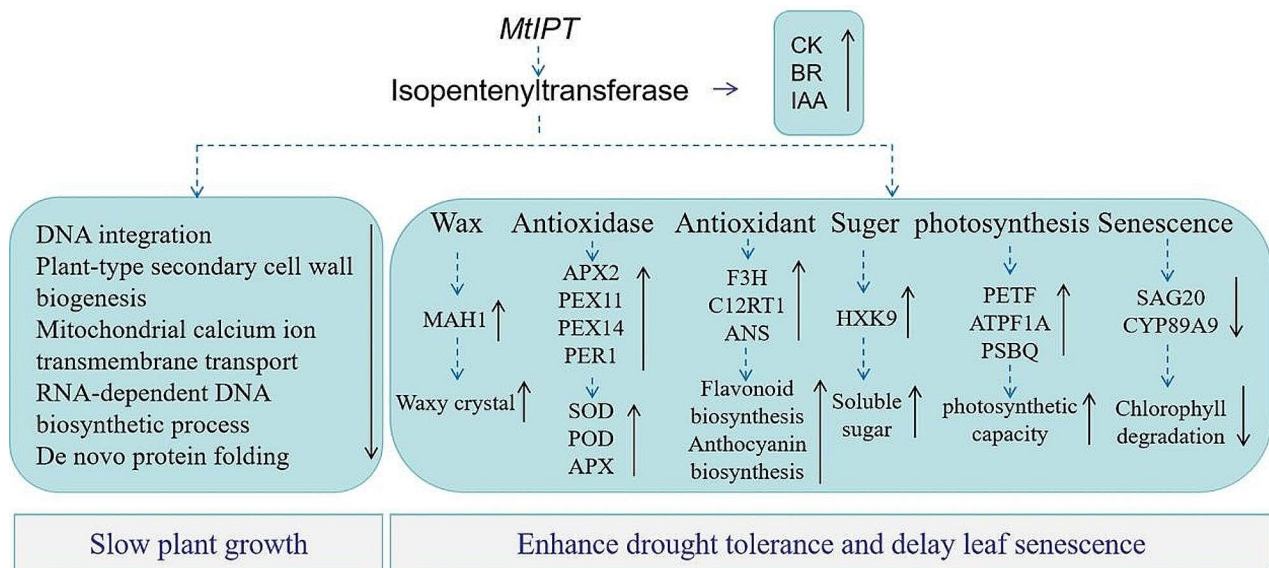


Fig. 11 A proposed working model of *MtIPT* in regulating plant growth, drought stress response and leaf senescence in *Agrostis stolonifera*. The dashed blue arrow indicates the corresponding relationship, the black up arrow indicates the up-regulating, and the black down arrow indicates the down-regulating

Epidermal wax forms a hydrophobic layer that coats the plant surface, crucial for maintaining water balance and preventing water loss [33, 34]. In this study, we observed that the *MtIPT* gene significantly increased the expression of the wax synthesis gene *MAHI* (Fig. 10D) and influenced the content and morphology of wax crystals around stomata (Fig. 3G) in OE plant leaves. This finding helps to reduce water loss and may be a key factor contributing to increased drought resistance in OE plants.

CRE1, *AHK2*, and *AHK3*, are CK signal transduction genes encoding arabidopsis histidine kinase that act as negative regulators in ABA signal transduction. Mutants *cer1*, *ahk2*, and *ahk3* in *Arabidopsis* exhibit enhanced drought tolerance [35]. CK signal transduction B-type ARR protein mediates drought response in *Arabidopsis* as a negative regulator, and the improved drought tolerance of *arr* mutant plants is associated with enhanced cell membrane integrity, increased anthocyanin biosynthesis, abscisic acid hypersensitivity, and decreased stomatal pore size [36]. In this study, compared with WT plants, the expression levels of *CER1*, *AHK2*, and *AHK3* genes were down-regulated, along with down-regulation of four B-type *ARR* genes and up-regulation of one in the CK signaling pathway of OE plants. This modulation may contribute significantly to the enhanced drought tolerance observed in OE plants.

Senescence-associated genes (*SAGs*) are pivotal in regulating leaf senescence. Cytochrome P450 *CYP89A9* participates in the formation of major chlorophyll catabolites during leaf senescence in plants [37]. Jing, et al. [38] demonstrated that melatonin suppressed age- and dark-induced leaf senescence in cucumber (*Cucumis sativus*) by reducing the expression of *SAG20* and the cell-death-related gene *PDCD*, while increasing antioxidant capacity and chlorophyll biosynthesis. In this study, compared with WT plants, the expression of *SAG20* (Fig. 10F) and cytochrome P450 *CYP89A9* (Fig. 10G) genes in OE plants were significantly decreased. Concurrently, genes related to photosynthesis (*ATPF1A*, *PSBQ*, *PETF*) and antioxidase-related genes were notably up-regulated in OE plants. Therefore, overexpression of the *MtIPT* gene likely delays leaf senescence by enhancing chlorophyll content, photosynthetic capacity, and antioxidant capacity in OE plants.

Plant hormones play critical roles in growth, development, and abiotic stress response through found complex interactions. Xia, et al. [39] demonstrated that brassinosteroids in tomato (*Solanum lycopersicum*) influence apical dominance by integrating signals from auxin, abscisic acid, gibberellin, and cytokinin, along with sugar signaling. Li, et al. [40] revealed that auxin, brassinosteroid, and cytokinin interact to regulate root meristem development, involving auxin signaling components like *PIN7* and *SHY2*. In this study, in addition to significant

increases in isopentenyl adenosine and trans-zeatin-riboside, the levels of auxin and brassinosteroid were significantly elevated in *MtIPT*-overexpressed plants. Moreover, the expression of the *MtIPT* gene increased notably upon exogenous EBR spraying, indicating that CKs influence auxin and brassinosteroid synthesis by regulating gene expression. Conversely, brassinosteroids can also affect CK synthesis, but further mechanistic studies are needed.

Brassinosteroids play crucial roles in plant response to abiotic stress. Chen, et al. [41] demonstrated that the brassinosteroid-deficient cotton mutant *pag1* (*pagoda1*) exhibited increased sensitivity to drought stress compared with wild-type plants. Chen, et al. [42] indicated that brassinosteroid enhanced the heat tolerance of plants by inhibiting *ERF49* expression through *BZR1*. Additionally, Liu, et al. [43] confirmed that brassinosteroid signal transduction plays a vital role in regulating plant salt tolerance through a series of *Arabidopsis* brassinosteroid mutant and overexpressed materials. In this study, changes in hormone levels strongly suggest that brassinosteroid variation is a critical aspect of *MtIPT* gene regulation in transgenic creeping bentgrass under abiotic stress conditions.

Conclusion

In conclusion, we have proposed a working model outlining the molecular mechanisms by which *MtIPT* regulates plant growth, drought stress response, and leaf senescence (Fig. 11). The *IPT* gene from *M. truncatula* was overexpressed in creeping bentgrass, resulting in observed slower growth of both aboveground and root parts, thinner leaves, and darker leaf color compared with WT plants. Physiological indices measured after drought and shade stress treatments demonstrated significantly enhanced drought resistance and improved shade tolerance in OE plants, achieved through delayed leaf senescence. The wax content in the leaf epidermis, critical for water retention, was found to be closely linked to these traits. Scanning electron microscope results revealed a notable increase in wax crystal content around the stomata of OE plants, contributing to reduced water loss under drought stress conditions. High-throughput sequencing uncovered numerous DEGs associated with growth, development, and response to abiotic stress, including those related to auxin signaling, root development, photosynthesis, and peroxisome function, among others. Importantly, the overexpression of the *MtIPT* gene not only increased the levels of cytokinins (isopentenyl adenosine and trans-zeatin-riboside) in OE plants but also significantly elevated auxin and brassinosteroid levels. These findings suggest that *MtIPT* influences the physiological changes in OE plants by regulating the interactions among various hormones. These results

provide valuable insights and a foundation for further exploration into the molecular mechanisms underlying the effects of the *IPT* gene on plant growth, development, and response to abiotic stresses. Additionally, they offer new avenues for genetic improvement of creeping bentgrass.

Material and method

MtIPT gene cloning, plasmid construction and plant transformation.

The material used in this study included *M. truncatula* R108 seeds obtained from the Noble Foundation in the United States. These seeds were planted in soil (vermiculite: nutrient soil: perlite=1:1:1) and cultivated for 2 months in a greenhouse to mature plants. Total RNA was extracted from *M. truncatula* leaves, and the *MtIPT* gene (XM_003590629.4), 903 bp, was cloned using PCR. Subsequently, the gene was ligated into the 3302-UBI vector containing the CaMV35S promoter to construct a plant expression vector. This vector was then introduced into the genome of the WT creeping bentgrass 'Penn A4' using the agrobacterium-mediated method, resulting in the generation of OE plants.

Subcellular localization of MtIPT protein.

Tobacco seeds were germinated under conditions similar to those used for *M. truncatula*. The *MtIPT* gene was cloned into the 3302Y vector, which contains the *YFP* gene, and subsequently transformed into *Agrobacterium* EHA105. The properties that *YFP* can be expressed in various subcellular structures can be used to study the localization of genes. When the tobacco plants reached 5–6 weeks of age, both the 3302Y vector and 3302Y-*MtIPT* construct were separately introduced into tobacco leaves using agrobacterium-mediated transformation. The reason for using 3302Y vector containing the *YFP* gene as a control is to distinguish between plant autofluorescence and YFP fluorescence to avoid spurious interference. After a two-day period of dark culture, subcellular localization was observed under the YFP channel of a confocal microscope. In order to facilitate observation, the fluorescence color was set to green in confocal microscopy.

Response of *MtIPT* gene to drought stress.

Four mature *M. truncatula* plants were carefully selected and subjected to drought treatment using 20% (w/v) PEG 6000, following the method described by [44, 45] with modifications. Samples were collected at intervals of 0 h, 0.5 h, 1 h, 2 h, 4 h, 6 h, 8 h, 12 h, and 24 h. At each time point, 0.1 g of *M. truncatula* leaves was rapidly frozen with liquid nitrogen and stored at -80 °C. Total RNA was extracted from the samples using the Trizol method and reverse-transcribed into cDNA for subsequent qRT-PCR analysis.

Plant materials, propagation and abiotic stress treatment.

WT and OE plants overexpressing *MtIPT* were transplanted from the growth medium into 15 cm × 15 cm pots filled with soil (vermiculite: nutrient soil: perlite=1:1:1) and placed under a 16 h/8 h light/dark cycle at 23 °C. After 12 weeks of growth, WT and OE plants were carefully removed from the pots and cleaned thoroughly. Observations were made on the growth of aboveground parts and roots, and measurements were taken for stem length, root length, leaf width, and chlorophyll content of the plants. Samples from WT, OE2, and OE16 plants were selected for measurement of these parameters, each with three biological replicates.

For the drought stress experiments, WT control and OE plants were planted in pots containing 200 g of soil, following the initial maintenance procedure described above. The soil field moisture capacity of each pot was measured according to the method described by Yuan [46] with modifications. After 12 weeks of growth, plants at similar developmental stages were chosen for drought treatment. Natural drought stress conditions were applied to ensure the authenticity and accuracy of physiological parameters. By the 14th day of drought treatment, the soil water content was calculated on the basis of soil field moisture capacity [47]. The water content of the soil planted with WT plants was measured as 34%, 32%, and 33% of field moisture capacity, while that of soil planted with OE2 plants was 33%, 32%, and 33% of field moisture capacity, and OE16 plants showed 34%, 33%, and 33% of field moisture capacity, respectively. Observations and photographs were taken daily to monitor leaf changes, and leaf samples were collected on days 0 and 14 of the treatment. These samples were rapidly frozen with liquid nitrogen and stored at -80 °C for subsequent analysis of chlorophyll content, soluble sugar content, MDA content, and antioxidant enzyme activities including POD, SOD, and APX. WT, OE2, OE7, and OE16 plants were selected as samples for measuring physiological parameters, each with three biological replicates.

Regarding the shade treatment, leaves of WT and OE plants under the same soil culture conditions mentioned above were cultured in vitro in 3 mM MES solution under dark conditions. MES is a zwitterionic buffer that mimics the plant's natural environment. Our laboratory previously determined through ion concentration gradient experiments that 3 mM MES is effective for the survival of creeping bentgrass. MES solution was used to simulate an in vitro leaf culture environment, and the plants were subjected to a light shading experiment. This method was chosen for its simplicity and ease of observation of experimental results. Daily observations and photographs were taken to monitor leaf changes, and chlorophyll content was measured on days 0, 5, and 8 of

the shading treatment. WT, OE2, OE16 leaves with the same growth state were selected from the three plants respectively as three biological repeat samples.

Tissue sections and scanning electron microscopy.

Paraffin transverse sections of creeping bentgrass leaves were prepared according to the method described by Yuan, et al. [48] with modifications. These sections were then stained with ferro red and green fixation to observe the cellular morphological structure of creeping bentgrass leaves under a light microscope (NIKON, Japan). Samples from WT, OE2, and OE16 plants were selected for sectioning, with each sample having three biological replicates.

Fresh plant leaves were fixed using an electron microscope fixative solution (Servicebiop, China), followed by post-fixation, dehydration, drying, and conductive treatment. The epidermal structure of the plant leaves was subsequently observed, and images were captured using SEM (HITACHI, China) [49]. Samples from WT, OE2, and OE16 plants were chosen for SEM imaging, each with three biological replicates.

Determination of chlorophyll content, soluble sugar content, antioxidant enzyme content and malondialdehyde content.

Chlorophyll content was measured following established protocols [50]. The activities of antioxidant enzymes, including POD, SOD and APX, were determined according to Nahakpam, et al. [51]. Malondialdehyde content was quantified using the method described by Esterbauer, et al. [52]. Plant soluble sugar content was assessed using the Plant Soluble Sugar Content Assay Kit following the manufacturer's instructions.

Hormone Contents Assay.

The leaves of 12-week old WT and OE plants were collected and crushed with liquid nitrogen immediately after rapid freezing. Hormone contents were measured following the method outlined by Dong, et al. [53]. Samples from WT, OE2, and OE16 were chosen, with each sample having three biological replicates. The calculation method adhered to protocols described previously [54].

Application of exogenous 24-epibrassinolide

Four mature plants of *M. truncatula* were carefully selected and sprayed with a 0.1 μ M solution of EBR following the method outlined by Yuan et al. (2012) with some modifications. Samples were collected at 0 h, 0.5 h, 1 h, 3 h, 6 h, 9 h, 12 h, and 24 h intervals. At each time point, 0.1 g of *M. truncatula* leaves was swiftly frozen with liquid nitrogen and stored at -80°C . Total RNA was extracted from the samples using the Trizol method and reverse-transcribed into cDNA for subsequent qRT-PCR analysis.

Statistical tests

The statistical data were visualized using Prism 9 software, and significance between the WT and OE samples was analyzed using the unpaired t-test.

RNA extraction and gene expression assay

Plant total RNA was extracted from 100 mg of fresh leaf, root, and shoot samples using the method described by Sun, et al. [15], with each sample consisting of four biological replicates. Real-time quantitative RT-PCR was performed following previously published protocols [15, 55]. The ubiquitin gene of creeping bentgrass, AsUBQ (JX570760), was used as a reference. The relative expression level of each gene was calculated using the $2^{-\Delta\Delta\text{Ct}}$ method [56, 57].

RNA-seq analysis

Total RNA was extracted from each sample and treated with gDNA Eraser (TaKaRa, Japan) to eliminate contaminating genomic DNA. Samples WT and OE2 were selected, with each sample comprising three biological replicates. Details on correlations and differences among the samples are provided in the supplementary materials (Fig. S3, S4).

RNA integrity and purity were assessed on 1% agarose gels and using a NanoPhotometer spectrophotometer (IMPLEN, USA). RNA concentration was measured with a Qubit RNA Assay Kit on a Qubit 2.0 Fluorometer (Life Technologies, USA), and RNA integrity was evaluated using the RNA Nano 6000 Assay Kit on the Bioanalyzer 2100 system (Agilent Technologies, USA). For library construction, 3 μ g of RNA per sample was used. Sequencing libraries were generated using the VAHTSTM Universal DNA Library Prep Kit for Illumina[®] V2 (NuoWeiZan, China), following the manufacturer's instructions, with index codes added to attribute sequences to each sample. Library quality was assessed using the Agilent Bioanalyzer 2100 system, and sequencing was conducted on a HiSeq4000 instrument.

After removing reads containing adapter sequences and filtering out low-quality reads from raw data, clean data were obtained and used for transcriptome analysis. RSEM was employed to estimate gene and isoform expression levels using the clean data, with the unigene sequence file as the reference gene file [58, 59]. DESeq2 software was utilized to analyze differentially expressed genes, using parameters of adjusted p -value < 0.01 and $|\log_2 \text{FC}| \geq 2$ [60].

Unigene sequences were aligned to various databases, including Nonredundant protein (NR), SwissProt, Pfam, Gene Ontology (GO), Cluster of Orthologous Groups (COG), Kyoto Encyclopedia of Genes and Genomes (KEGG), Evolutionary Genealogy of Genes: Non-supervised Orthologous Groups Database (eggNOG), and

Cluster of Orthologous Groups (KOG/COG) databases [61, 62]. GO annotation was performed using Blast2GO software (version 2.3.5). The KEGG Automatic Annotation Server (KAAS1) was used for KEGG pathway annotation, and the Pfam database was searched using HMMER software (Eddy 1998).

Supplementary Information

The online version contains supplementary material available at <https://doi.org/10.1186/s12870-024-05442-5>.

Supplementary Material 1
Supplementary Material 2
Supplementary Material 3
Supplementary Material 4
Supplementary Material 5
Supplementary Material 6
Supplementary Material 7
Supplementary Material 8
Supplementary Material 9
Supplementary Material 10
Supplementary Material 11

Acknowledgements

Ye Ai acknowledges the support of the China Scholarship Council for her academic visit to the University of Western Australia. Yinglong Chen was supported by the Australian Research Council (FT210100902).

Author contributions

L.H., Y.Chao, and Y.A. contributed to the concept and design of the study. Y.A. completed major experimental work, data analysis and wrote the first draft of the manuscript. N.W. assisted in the figure preparation. J.Li., J.Liu, and L.S. assisted with some of the experimental work. L.H., Y.Chen., Y.Chao, and X.S. revised the manuscript. All authors read and approved the final manuscript.

Funding

This work was supported by National Key Research and Development Program of China [grant number 2023YFD1200302]; 5.5 Engineering Research & Innovation Team Project of Beijing Forestry University [grant number BLRC2023A04].

Data availability

The original data obtained from transcriptome sequencing have been uploaded to NCBI database at the login number PRJNA1082913: <https://www.ncbi.nlm.nih.gov/sra/PRJNA1082913>.

Declarations

Ethics approval and consent to participate

The experimental research on plants complied with relevant institutional, national and international guidelines and legislation, and all methods were performed in accordance with the relevant guidelines and regulations.

Consent for publication

Not applicable.

Competing interests

The authors declare no competing interests.

Supplementary Information

Additional file 1:

Table S1 The biological process analysis of Gene Ontology enrichment of the all annotated differentially expressed genes.
Table S2 The biological process analysis of Gene Ontology enrichment of the up-regulated differentially expressed genes.
Table S3 The biological process analysis of Gene Ontology enrichment of the down-regulated differentially expressed genes.
Table S4 The cellular component analysis of Gene Ontology enrichment of the all annotated differentially expressed genes.
Table S5 The cellular component analysis of Gene Ontology enrichment of the up-regulated differentially expressed genes.
Table S6 The cellular component analysis of Gene Ontology enrichment of the down-regulated differentially expressed genes.
Table S7 The molecular function analysis of Gene Ontology enrichment of the all annotated differentially expressed genes.
Table S8 The molecular function analysis of Gene Ontology enrichment of the up-regulated differentially expressed genes.
Table S9 The molecular function analysis of Gene Ontology enrichment of the down-regulated differentially expressed genes.
Additional file 2:

Received: 28 May 2024 / Accepted: 22 July 2024

Published online: 01 August 2024

References

- Lacuesta M, Saiz-Fernández I, Podlešáková K, Miranda-Apodaca J, Novák O, Doležal K, Diego ND. The *trans* and *cis* zeatin isomers play different roles in regulating growth inhibition induced by high nitrate concentrations in maize. *Plant Growth Regul.* 2018; 85(2):199–209.
- Skoog F, Miller CO. Chemical regulation of growth and organ formation in plant tissues cultured in vitro. *Symp Soc Exp Biol.* 1957;11:118–30.
- Zhao J, Ding B, Zhu E, Deng X, Zhang M, Zhang P, et al. Phloem unloading via the apoplastic pathway is essential for shoot distribution of root-synthesized cytokinins. *Plant Physiol.* 2021;186(4):2111–23.
- Sakakibara H. Cytokinins: activity, biosynthesis, and translocation. *Annu Rev Plant Biol.* 2006;57:431–49.
- Van Staden J, Dimalla GG. The effect of silver thiosulphate preservative on the physiology of cut carnations II. Influence on endogenous cytokinins. *Z für Pflanzenphysiologie.* 1980;99(1):19–26.
- Zhang W, Peng K, Cui F, Wang D, Zhao J, Zhang Y, et al. Cytokinin oxidase/dehydrogenase OsCKX11 coordinates source and sink relationship in rice by simultaneous regulation of leaf senescence and grain number. *Plant Biotechnol J.* 2021;19(2):335–50.
- Barry GF, Rogers SG, Fraley RT, Brand L. Identification of a cloned cytokinin biosynthetic gene. *Proc Natl Acad Sci USA.* 1984;81(15):4776–80.
- Kakimoto T. Biosynthesis of cytokinins. *J Plant Res.* 2003;116(3):233–9.
- Lindner AC, Lang D, Seifert M, Podlešáková K, Novák O, Strnad M, Reski R, Schwartzberg KV. Isopentenyltransferase-1 (IPT1) knockout in *Physcomitrella* together with phylogenetic analyses of IPTs provide insights into evolution of plant cytokinin biosynthesis. *J Exp Bot.* 2014;65(9):2533–43.
- McKenzie MJ, Jameson PE, Poulter RTM. Cloning an *ipt* gene from *Agrobacterium tumefaciens*: characterisation of cytokinins in derivative transgenic plant tissue. *Plant Growth Regul.* 1994;14(3):217–28.
- Hewelt A, Prinsen E, Schell J, Onckelen HV, Schmölling T. Promoter tagging with a promoterless *ipt* gene leads to cytokinin-induced phenotypic variability in transgenic tobacco plants: implications of gene dosage effects. *Plant J.* 1994;6(6):879–91.
- Belintani NG, Guerzoni JTS, Moreira RMP, Vieira LGE. Improving low-temperature tolerance in sugarcane by expressing the *ipt* gene under a cold inducible promoter. *Biol Plant.* 2012;56(1):71–7.
- Qin H, Gu Q, Zhang JL, Sun L, Kuppu S, Zhang YZ, et al. Regulated expression of an isopentenyltransferase gene (*IPT*) in peanut significantly improves Drought Tolerance and increases yield under field conditions. *Plant Cell Physiol.* 2011;52(11):1904–14.
- Liu YD, Yin ZJ, Yu JW, Li J, Wei HL, Han XL, Shen FF. Improved salt tolerance and delayed leaf senescence in transgenic cotton expressing the *Agrobacterium IPT* gene. *Biol Plant.* 2012;56(2):237–46.
- Sun X, Huang N, Li X, Zhu J, Bian X, Li H, Wang L, Hu Q, Luo H. A chloroplast heat shock protein modulates growth and abiotic stress response in creeping bentgrass. *Plant Cell Environ.* 2021;44(6):1769–87.

16. Han RH, Li ZD, Gao GJ, Chen P, Shi XL, Zhou YL, Wang MZ. Research progress on creeping stolon of superior lawn grass. *Guangdong Agric Sci.* 2011;38(15):39–42.
17. Merewitz EB, Gianfagna T, Huang B. Protein accumulation in leaves and roots associated with improved drought tolerance in creeping bentgrass expressing an *ipt* gene for cytokinin synthesis. *J Exp Bot.* 2011;62(15):5311–33.
18. Xu Y, Burgess P, Zhang X, Huang B. Enhancing cytokinin synthesis by overexpressing *ipt* alleviated drought inhibition of root growth through activating ROS-scavenging systems in *Agrostis stolonifera*. *J Exp Bot.* 2016;67:1979–92.
19. Sa G, Mi M, Ye HC, Li GF. Anther-specific expression of *ipt* gene in transgenic tobacco and its effect on plant development. *Transgenic Res.* 2002;11(3):269–78.
20. Ye CJ, Wu SW, Kong FN, Zhou CJ, Yang QK, Sun Y, Wang B. Identification and characterization of an isopentenyltransferase (*ipt*) gene in soybean (*Glycine max* L). *Plant Sci.* 2006;170(3):542–50.
21. Skalák J, Černý M, Jedelský P, Dobrá J, Ge E, Novák J, et al. Stimulation of *ipt* overexpression as a tool to elucidate the role of cytokinins in high temperature responses of *Arabidopsis thaliana*. *J Exp Bot.* 2016;67(9):2861–73.
22. Shan Y, Zhao P, Liu Z, Li F, Tian X. An isopentenyl transferase gene driven by the senescence-inducible *SAG12* promoter improves salinity stress tolerance in cotton. *J Cotton Res.* 2019;2(1):15.
23. Xu Y, Huang BR. Transcriptional factors for stress signaling, oxidative protection, and protein modification in *ipt*-transgenic creeping bentgrass exposed to drought stress. *Environ Exp Bot.* 2017;144:49–60.
24. Hu X, Zhang A, Zhang J, Jiang M. Abscisic acid is a key inducer of hydrogen peroxide production in leaves of maize plants exposed to water stress. *Plant Cell Physiol.* 2006;47(11):1484–95.
25. Volkov RA, Panchuk II, Mullineaux PM, Schöffl F. Heat stress-induced H₂O₂ is required for effective expression of heat shock genes in *Arabidopsis*. *Plant Mol Biol.* 2006;61(4–5):733–46.
26. Ozkur O, Ozdemir F, Bor M, Turkan I. Physicochemical and antioxidant responses of the perennial xerophyte *Capparis ovata* Desf. to drought. *Environ Exp Bot.* 2009;66(3):487–92.
27. Nessa F, Ismail Z, Mohamed N, Haris MRHM. Free radical-scavenging activity of organic extracts and of pure flavonoids of *Blumea balsamifera* DC leaves. *Food Chem.* 2004;88(2):243–52.
28. Proestos C, Boziaris IS, Nychas GJE, Komaitis M. Analysis of flavonoids and phenolic acids in Greek aromatic plants: investigation of their antioxidant capacity and antimicrobial activity. *Food Chem.* 2006;95(4):664–71.
29. Landi M, Tattini M, Gould KS. Multiple functional roles of anthocyanins in plant-environment interactions. *Environ Exp Bot.* 2015;119:4–17.
30. Noguez S, Allen DJ, Morison JI, Baker NR. Ultraviolet-B radiation effects on water relations, leaf development, and photosynthesis in droughted pea plants. *Plant Physiol.* 1998;117(1):173–81.
31. Offen W, Martinez-Fleites C, Yang M, Kiat-Lim E, Davis BG, Tarling CA, Ford CM, Bowles DJ, Davies GJ. Structure of a flavonoid glucosyltransferase reveals the basis for plant natural product modification. *EMBO J.* 2006;25(6):1396–405.
32. Saito K, Kobayashi M, Gong Z, Tanaka Y, Yamazaki M. Direct evidence for anthocyanidin synthase as a 2-oxoglutarate-dependent oxygenase: molecular cloning and functional expression of cDNA from a red form of *Perilla frutescens*. *Plant J.* 1999;17(2):181–9.
33. Seo PJ, Lee SB, Mi CS, Park MJ, Go YS, Park CM. The MYB96 transcription factor regulates cuticular wax biosynthesis under drought conditions in *Arabidopsis*. *Plant Cell.* 2011;23(7):1138–52.
34. Tafolla-Arellano JC, Báez-Sañudo R, Tiznado-Hernández WE. The cuticle as a key factor in the quality of horticultural crops. *Sci Hortic.* 2018;232:145–52.
35. Tran L-SP, Urao T, Qin F, Maruyama K, Kakimoto T, Shinozaki K, Yamaguchi-Shinozaki K. Functional analysis of *AHK1/ATHK1* and cytokinin receptor histidine kinases in response to abscisic acid, drought, and salt stress in *Arabidopsis*. *Proc Natl Acad Sci USA.* 2007;104(51):20623–8.
36. Argyros RD, Mathews DE, Chiang Y-H, Palmer CM, Thibault DM, Etheridge N, et al. Type B response regulators of *Arabidopsis* Play Key roles in Cytokinin Signaling and Plant Development. *Plant Cell.* 2008;20(8):2102–16.
37. Christ B, Süßenbacher I, Moser S, Bichsel N, Egert A, Müller T, Kräutler B, Hörtensteiner S. Cytochrome P450 CYP89A9 is involved in the formation of major chlorophyll catabolites during leaf senescence in *Arabidopsis*. *Plant Cell.* 2013;25(5):1868–80.
38. Jing T, Liu K, Wang Y, Ai X, Bi H. Melatonin positively regulates both dark- and Age-Induced Leaf Senescence by reducing ROS Accumulation and modulating Abscisic Acid and Auxin Biosynthesis in Cucumber plants. *Int J Mol Sci.* 2022;23(7).
39. Xia XJ, Dong H, Yin YL, Song XW, Gu XH, Sang KQ, et al. Brassinosteroid signaling integrates multiple pathways to release apical dominance in tomato. *Proc Natl Acad Sci USA.* 2021;118(11).
40. Li TT, Kang XK, Lei W, Yao XH, Zou LJ, Zhang DW, Lin HH. SHY2 as a node in the regulation of root meristem development by auxin, brassinosteroids, and cytokinin. *J Integr Plant Biol.* 2020;62(10):1500–17.
41. Chen EY, Zhang XY, Yang ZR, Zhang CJ, Wang XQ, Ge XY, Li FG. BR deficiency causes increased sensitivity to drought and yield penalty in cotton. *BMC Plant Biol.* 2019;19(1):220.
42. Chen X, Xue H, Zhu L, Wang H, Long H, Zhao J, et al. ERF49 mediates brassinosteroid regulation of heat stress tolerance in *Arabidopsis thaliana*. *BMC Biol.* 2022;20(1):254.
43. Liu JL, Yang RC, Jian N, Wei L, Ye LL, Wang RH, Gao HL, Zheng QS. Putrescine metabolism modulates the biphasic effects of brassinosteroids on canola and *Arabidopsis* salt tolerance. *Plant Cell Environ.* 2020;43(6):1348–59.
44. Castañeda V, González EM. Strategies to apply water-deficit stress: similarities and disparities at the whole plant metabolism level in *Medicago truncatula*. *Int J Mol Sci.* 2021;22(6).
45. Elmaghribi AM, Rogers HJ, Francis D, Ochatt SJ. PEG induces high expression of the cell cycle checkpoint gene *WEE1* in Embryogenic Callus of *Medicago truncatula*: potential link between cell cycle checkpoint regulation and osmotic stress. *Front Plant Sci.* 2017;8:1479.
46. Yuan N. Soil field water capacity was determined by indoor ring knife method. *China New Technol Prod.* 2014;9(1).
47. Kirkham MB. Chapter 4 - Soil-water terminology and applications. In: Kirkham MB. Principles of Soil and Plant Water Relations (Third Edition). Academic Press; 2023. pp. 49–63.
48. Yuan S, Li Z, Li D, Yuan N, Hu Q, Luo H. Constitutive expression of Rice *MicroRNA528* alters Plant Development and enhances tolerance to Salinity Stress and Nitrogen Starvation in creeping Bentgrass. *Plant Physiol.* 2015;169:576–93.
49. Akhtar K, Khan SA, Khan SB, Asiri AM. Scanning Electron Microscopy: Principle and Applications in nanomaterials characterization. Sharma SK. Handbook of materials characterization. Cham: Springer International Publishing; 2018. pp. 113–45.
50. Li Z, Baldwin CM, Hu Q, Liu H, Luo H. Heterologous expression of *Arabidopsis* H⁺-pyrophosphatase enhances salt tolerance in transgenic creeping bentgrass (*Agrostis stolonifera* L). *Plant Cell Environ.* 2010;33(2):272–89.
51. Nahakpam S, Shah K. Expression of key antioxidant enzymes under combined effect of heat and cadmium toxicity in growing rice seedlings. *Plant Growth Regul.* 2011;63(1):23–35.
52. Esterbauer H, Cheeseman KH. Determination of aldehydic lipid peroxidation products: Malonaldehyde and 4-hydroxynonenal. In: Methods Enzymol. Academic Press; 1990. pp. 407–421.
53. Dong D, Yang Z, Ma Y, Li S, Wang M, Li Y, et al. Expression of a Hydroxycinnamoyl-CoA Shikimate/Quinate Hydroxycinnamoyl Transferase 4 gene from *Zoysia japonica* (*ZjHCT4*) causes excessive elongation and lignin composition changes in *Agrostis stolonifera*. *Int J Mol Sci.* 2022;23(16):9500.
54. Zhao J, Li G, Yi GX, Wang BM, Deng AX, Nan TG, Li ZH, Li QX. Comparison between conventional indirect competitive enzyme-linked immunosorbent assay (icELISA) and simplified icELISA for small molecules. *Anal Chim Acta.* 2006;571(1):79–85.
55. Li S, Fu Q, Chen L, Huang W, Yu D. *Arabidopsis thaliana* WRKY25, WRKY26, and WRKY33 coordinate induction of plant thermotolerance. *Planta.* 2011;233(6):1237–52.
56. Livak K. Relative quantitation of gene expression. London: UCL; 2001.
57. Zhou M, Li D, Li Z, Hu Q, Yang C, Zhu L, Luo H. Constitutive expression of a *mir319* gene alters plant development and enhances salt and drought tolerance in transgenic creeping bentgrass. *Plant Physiol.* 2013;161(3):1375–91.
58. Fu L, Niu B, Zhu Z, Wu S, Li W. CD-HIT: accelerated for clustering the next-generation sequencing data. *Bioinformatics.* 2012;28(23):3150–2.
59. Li B, Dewey CN. RSEM: accurate transcript quantification from RNA-Seq data with or without a reference genome. *BMC Bioinform.* 2011;12:323.
60. Chao YH, Xie LJ, Yuan JB, Guo T, Li YRZ, Liu FQ, Han LB. Transcriptome analysis of leaf senescence in red clover (*Trifolium pratense* L). *Physiol Mol Biol Plants.* 2018;24(Suppl 1):1–13.
61. Minoru K, Susumu G, Shuichi K, Yasushi O, Masahiro H. The KEGG resource for deciphering the genome. *Nucleic Acids Res.* 2004;32(Database issue):D277–80.
62. Tatusov RL, Galperin MY, Natale DA, Koonin EV. The COG database: a tool for genome-scale analysis of protein functions and evolution. *Nucleic Acids Res.* 2000;28(1):33–6.

Publisher's Note

Springer Nature remains neutral with regard to jurisdictional claims in published maps and institutional affiliations.